# Influence of *p*-Type Double-Doping on the Crystals and Electronic Structures of Two Polar Intermetallics: $La_{4.57(1)}Li_{0.43}Ge_{3.80(3)}In_{0.20}$ and $Nd_{4.32(1)}Li_{0.68}Ge_{3.87(3)}In_{0.13}$

**Jieun Jeon, Junsu Lee, and Tae-Soo You***

*Department of Chemistry, Chungbuk National University, Cheongju 28644, Republic of Korea.*
**E-mail: tsyou@chungbuk.ac.kr*
*Received June 21, 2018, Accepted July 9, 2018*

Two quaternary polar intermetallic compounds $La_{4.57(1)}Li_{0.43}Ge_{3.80(3)}In_{0.20}$ and $Nd_{4.32(1)}Li_{0.68}Ge_{3.87(3)}In_{0.13}$ were synthesized using a conventional high temperature synthetic method as we attempted to introduce the *p*-type double-doping of Li and In for RE and Ge in the $RE_{5-x}Li_xGe_{4-y}$ (RE = rare-earth metals) system, and their crystal structures were characterized by single crystal X-ray diffraction experiments. The two title compounds crystallize in the orthorhombic space group *Pnma* (Pearson code *oP*16, $Z = 4$) with six crystallographically independent asymmetric atomic sites and adopt the $Gd_5Si_4$-type structure. Overall crystal structures of two isotypic title compounds can be described as a 1:1 assembly of the hypothetical 2-dimensional (2D) $RE_2(RE/Li)(In/Ge)_2$ layered structure adopting the $Mo_2FeB_2$-type structure and the dumbbell-shaped inter-slab $(In/Ge)_2$ dimers bridging two such neighboring 2D layers along the crystallographic *b*-axis direction. The observed "direction selective" structural transformation from the $Sm_5Ge_4$-type to the $Gd_5Si_4$-type structure can be understood as a result of the simultaneous double-doping by the relatively smaller amount of Li substitution for La at the RE3 site than that in the $La_4LiGe_4$ and the partial In substitution for Ge at both of the *M*1 and *M*3 sites. The site-preference of In for two particular anionic sites were thoroughly studied using four hypothetical $La_4LiGe_3In$ models having different atomic arrangements by the tight-binding linear muffin-tin orbital (TB-LMTO) method. The overall electronic structure and individual chemical bonding influenced by the given double-doping were also discussed on the basis of the density of states (DOS) and crystal orbital Hamilton population (COHP) curves analyses.

**Keywords:** Polar intermetallics, Giant magnetocaloric effect, Single-crystal X-ray diffraction, Atomic site-preference, Electronic structure

## Introduction

Since $Gd_5Si_2Ge_2$ successfully demonstrated the giant magnetocaloric effect (MCE)[1] around room temperature, the great numbers of research activities on the related $RE_5Tt_4$ (RE = rare-earth metals, Tt = tetrels) series[2–4] have been conducted worldwide, and various derivatives belonging to this series of compounds have been reported. These experimental and theoretical investigations not only enhanced the giant MCE properties, but eventually help to understand the correlation among structure-composition-physical properties.[5–9] In particular, various cationic and anionic elemental substitution have been attempted, and some of the results of those trials include the $Gd_{5-x}Y_xTt_4$ (Tt = Si, Ge; $0 \le x \le 4$),[10] $Gd_{5-x}RE_xGe_4$ (RE = La, Lu; $0.05 \le x \le 0.4$ for La, $x = 0.125$, 0.25 for Lu),[11,12] $Gd_{5-x}Eu_xGe_4$ ($0 \le x \le 2$),[8,13] $Gd_{5-x}M_xTt_4$ (*M* = Zr, Hf; *Tt* = Si, Ge; $0.5 \le x \le 5$),[14] $La_{5-x}Y_xSi_4$ ($0 \le x \le 5$),[3] and $RE_{5-x}Mg_xGe_4$ (RE = Gd-Tm, Lu, Y; $1.0 \le x \le 2.3$) systems[15] for cation substitution, and $Gd_5Si_{1.5}Ge_{2.5}$,[16] the $Gd_5Ge_{4-x}Si_x$ ($0 \le x \le 3$),[17,18] $Gd_5Ge_{4-x}Ga_x$ ($0 \le x \le 2.2$),[19] and $Gd_5Si_{4-x}Sn_x$ ($0 \le x \le 3$) systems[20] for anion substitutions. Our research group also recently reported results of our systematic investigations for the *p*-type Li substituted $RE_4LiGe_4$ (RE = La, Ce, Pr, Sm) system.[21] In this work, we proved that the observed structural transformation was caused by both the chemical pressure[15] and the reduced valence electron count (VEC) descended from the *p*-type Li doping for RE, and the site-preference of Li for the RE3-site was nicely explained by the coloring-problem[22] on the basis of *q*-value (QVAL)[10] criterion.

In this work, we report our experimental and theoretical investigations for two quaternary polar intermetallic compounds $La_{4.57(1)}Li_{0.43}Ge_{3.80(3)}In_{0.20}$ and $Nd_{4.32(1)}Li_{0.68}Ge_{3.87(3)}In_{0.13}$, which can be considered as derivatives of the simultaneous *p*-type Li and In double-doping for RE and Ge, respectively, in the parental $RE_5Ge_4$ system. The "direction selective" structural transformation from the $Sm_5Ge_4$-type[23] to the $Gd_5Si_4$-type[24] structure caused by the *p*-type double-doping as well as the site-preference of anionic In and Ge were thoroughly investigated. In addition, a series of theoretical calculations were performed using four different structural models by TB-LMTO

  

method to understand the observed site-preference. An overall electronic structure including individual chemical bonding between anionic elements in the representative $La_3LiGe_3In$ was also thoroughly studied by using density of states (DOS) and crystal orbital Hamilton population (COHP) curves.

## Experimental

**Synthesis.** All of the sample preparation processes were performed inside a $N_2$-filled glovebox with $O_2$ and $H_2O$ contents below 0.1 ppm or inside an arc-melting furnace under vacuum. The reactant elements were purchased from Alfa Aesar (Karlsruhe, Germany) or Aldrich (Milwaukee, WI, USA): La (pieces, 99.9%), Nd (ingot, 99.9%), In (shot, 99.99%), Li (wire, 99.8%), and Ge (ingot, 99.9999%). Rare-earth metals and Li were cleaned by scrapping-off the lightly tanned surfaces using a scalpel or a metal brush inside a glovebox before used for reactions. Two title compounds were synthesized by the high-temperature reaction method using a Nb ampoule (diameter = 1 cm, length = 4 cm) and a muffle furnace. The reactants were cut into small pieces and loaded in the one end-sealed Nb ampoule inside a glovebox with the RE/Li/Ge/In ratio of 4: 1: 3: 1. The other end of the ampule was sealed by arc-welding under the Ar atmosphere. Then, this Nb ampule was sealed again in a secondary container of a fused-silica jacket under vacuum to prevent a Nb ampoule from the oxidation during the high-temperature reaction process. The reactant mixtures were heated to 1353 K at a rate of 273 K/h, kept there for 5 h, and then cooled to 1023 K at a rate of 10 K/h, where these products were annealed for 2 days. After then, the reactions were naturally cooled down to room temperature by turning off the furnace.

**X-Ray Diffraction Experiments.** Two title compounds $La_{4.57(1)}Li_{0.43}Ge_{3.80(3)}In_{0.20}$ and $Nd_{4.32(1)}Li_{0.68}Ge_{3.87(3)}In_{0.13}$ were characterized by both powder and single-crystal X-ray diffraction (PXRD and SXRD) analysis. PXRD patterns of title compounds were collected at room temperature using a Bruker D8 (Ettlingen, Germany) diffractometer equipped with an area detector and monochromatic Cu $K\alpha_1$ radiation ($\lambda$ = 1.54059 Å). The collection step size was set at 0.05° in the range of $15° \le 2\theta \le 85°$ with a total exposure time of 1 h. The phase purities of these title compounds were checked by comparing the collected PXRD patterns with the simulated patterns generated using SXRD data of the same title compounds. Both of these products contain small amounts of impurity phases including NdLiGe (see Figure S1, Supporting information). SXRD data were collected at room temperature using a Bruker SMART APEX2 CCD-based diffractometer equipped with Mo $K\alpha_1$ radiation ($\lambda$ = 0.71073 Å). Initially, several metallic silver needle/bar-shaped single crystals were chosen from each batch of products. After the quality check, the best single crystal was carefully selected, and a full data collection was conducted using Bruker's *APEX2* program.[25] Data reduction, integration, and unit cell parameter refinements were executed using the *SAINT* program.[26] *SADABS*[27] was used to perform semiempirical absorption corrections based on equivalents. The entire sets of reflections of two title compounds were in good agreements with the orthorhombic crystal system, and the space group *Pnma* (No. 62) was chosen for these two isotypic polar intermetallics. The detailed crystal structures were solved by direct method and refined to convergence by full matrix least-squares methods on $F^2$. The refined parameters of these $Gd_5Si_4$-type[24] phases include the scale factor, atomic positions including anisotropic displacement parameters (ADPs), extinction coefficients, and occupancy factors of the La/Li and Ge/In-mixed sites. During the last stage of this structure refinement cycle, each atomic position was standardized using *STRUCTURE TIDY*.[28] Important crystallographic data, atomic positions with ADPs and several selected interatomic distances are provided in Tables 1–3. Further details about each crystal structure can be obtained from the Fachinformationszentrum Karlsruhe, 76344 Eggenstein-Leopoldshafen, Germany (fax: (49) 7247–808-666; e-mail: crysdata@fiz-karlsruhe.de)—under depository numbers CSD-434513 for $La_{4.57(1)}Li_{0.43}Ge_{3.80(3)}In_{0.20}$ and CSD-434512 for $Nd_{4.32(1)}Li_{0.68}Ge_{3.87(3)}In_{0.13}$.

**Electronic Structure Calculations.** To understand the site-preference of anionic In over three available anionic

**Table 1.** SXRD data and structure refinement results for $La_{4.57(1)}Li_{0.43}Ge_{3.80(3)}In_{0.20}$ and $Nd_{4.32(1)}Li_{0.68}Ge_{3.87(3)}In_{0.13}$.

| | $La_{4.57(1)}Li_{0.43}Ge_{3.80(3)}In_{0.20}$ | $Nd_{4.32(1)}Li_{0.68}Ge_{3.87(3)}In_{0.13}$ |
|---|---|---|
| Formula weight (g/mol) | 936.38 | 923.79 |
| Space group; $Z$ | *Pnma* (No. 62; 4) | |
| Lattice parameters (Å) | $a$ = 7.8280(8)<br>$b$ = 15.639(2)<br>$c$ = 8.2084 (9) | $a$ = 7.5036(5)<br>$b$ = 15.1691 (12)<br>$c$ = 7.9657(6) |
| Volume (Å$^3$) | 1004.9 | 906.68 |
| $d_{calcd}$ (g/cm$^3$) | 6.189 | 6.768 |
| $\theta$ range for data collection | 2.61–25.67° | 2.69–24.70° |
| Independent reflections | 994 | 798 |
| Data/restraints/parameters | 994/0/49 | 798/0/49 |
| $R^a$ indices ($I > 2\sigma_I$) | $R_1$ = 0.0264<br>$wR_2$ = 0.0515 | $R_1$ = 0.0299<br>$wR_2$ = 0.0426 |
| $R^a$ indices (all data) | $R_1$ = 0.0404<br>$wR_2$ = 0.0550 | $R_1$ = 0.0464<br>$wR_2$ = 0.0506 |
| GOF on $F^2$ | 1.069 | 1.011 |
| Largest diff. of peak/hole (e/Å$^3$) | 1.437/−1.304 | 1.686/−1.480 |

[a] $R_1 = \Sigma||F_o| - |F_c||/\Sigma|F_o|$; $wR_2 = (\Sigma(w(F_o^2 - F_c^2)/\Sigma(w(F_o^2)^2))^{1/2}$, where $w = 1/(\sigma^2 F_o^2 + (A - P)^2 + B - P)$, and $P = (F_o^2 + 2F_c^2)/3$; $A$ and $B$—weight coefficients.

  

**Table 2.** Atomic coordinates and equivalent isotropic displacement parameters ($U_{eq}$[a]) from the SXRD refinements for $La_{4.57(1)}Li_{0.43}Ge_{3.80(3)}In_{0.20}$ and $Nd_{4.32(1)}Li_{0.68}Ge_{3.87(3)}In_{0.13}$.

| Atom | *Wyckoff* Site | Occupation | *x* | *y* | *z* | $U_{eq}$[a] (Å$^2$) |
|---|---|---|---|---|---|---|
| $La_{4.57(1)}Li_{0.43}Ge_{3.80(3)}In_{0.20}$ | | | | | | |
| La1 | 8d | 1 | 0.02578(7) | 0.59970(3) | 0.18542(6) | 0.01450(16) |
| La2 | 8d | 1 | 0.32047(7) | 0.12436(3) | 0.17942(6) | 0.01392(16) |
| La3/Li1 | 4c | 0.567(3)/0.433 | 0.14836(16) | 1/4 | 0.51050(15) | 0.0136(5) |
| *M*1[b] | 8d | 0.923(8)/0.077 | 0.15247(12) | 0.03817(6) | 0.47032(11) | 0.0159(3) |
| Ge2 | 4c | 1 | 0.02032(17) | 1/4 | 0.09136(17) | 0.0154(3) |
| *M*3[b] | 4c | 0.951(12)/0.049 | 0.26465(17) | 1/4 | 0.87029(15) | 0.0120(5) |
| $Nd_{4.32(1)}Li_{0.68}Ge_{3.87(3)}In_{0.13}$ | | | | | | |
| Nd1 | 8d | 1 | 0.02069(8) | 0.59886(4) | 0.18568(9) | 0.01035(18) |
| Nd2 | 8d | 1 | 0.32560(8) | 0.12629(4) | 0.17862(8) | 0.01032(18) |
| Nd3/Li1 | 4c | 0.320(3)/0.680 | 0.1519 (3) | 1/4 | 0.5102(3) | 0.0088(9) |
| *M*1[b] | 8d | 0.964(9)/0.036 | 0.15915(16) | 0.03690(8) | 0.46809(15) | 0.0124(5) |
| Ge2 | 4c | 1 | 0.0203(2) | 1/4 | 0.0873(2) | 0.0121(4) |
| *M*3[b] | 4c | 0.941(11)/0.059 | 0.2727 (2) | 1/4 | 0.8668(2) | 0.0101(6) |

[a] $U_{eq}$ is defined as one-third of the trace of the orthogonalized $U_{ij}$ tensor.
[b] *M* = Ge and In mixed-site.

sites as well as the overall electronic structure including individual chemical bonding, a series of theoretical calculations were conducted using four hypothetical structure models by the Stuttgart *TB-LMTO* 47 program[29–33] with the atomic sphere approximation (ASA). Since the two title compounds were isotypic, we used the La compound as a calculation model, and for practical reasons, the idealized composition of $La_4LiGe_3In$ was applied for these models. In order to apply two different atomic arrangements between In and Ge along the *b*-axis direction as In occupied the *M*1 site, two subgroups, *e.g.*, $P2_12_12_1$ (No. 19) and $P2_1/m$ (No. 11), of the refined space group *Pnma* were used for Model 1 and 2, respectively. For Model 2 and 3, where In occupies the *M*2 and *M*3 site, respectively, the experimentally refined space group *Pnma* (No. 62) was applied. Lattice parameters and atomic coordinates were extracted for the SXRD data of $La_{4.57(1)}Li_{0.43}Ge_{3.80(3)}In_{0.20}$. Further details about the structure models are provided in Table S1 (Supporting information). In the ASA method, space is filled with overlapping Wigner-Seitz (WS) atomic spheres.[29–33] All relativistic effects, except spin-orbit coupling, were taken into account using a scalar relativistic approximation. The symmetry of the potential inside each WS sphere was considered spherical, and a combined correction was used to take into account the overlapping part. The radii of WS sphere were obtained by requiring the overlapping potential be the best possible approximation to the full potential and were determined by an automatic procedure.[29–33] This overlap should not be too large because the error in kinetic energy introduced by the combined correction is proportional to the fourth power of the relative sphere overlap. The used WS radii for $La_4LiGe_3In$ are listed as follows: La = 1.838–2.097 Å, Li = 1.895 Å, Ge = 1.461–1.475 Å, and In = 1.534 Å. The basis sets included 6s, 6p, 5d, and 4f orbitals for La; 2s, 2p, and 3d orbitals for Li; 4s, 4p, and 4d orbitals for Ge; and 5s, 5p, 5d, and 4f orbitals for In. The La 6p, Li 2p, and 3d, Ge 4d and In 5d and 4f orbitals were treated by the Löwdin downfolding technique.[34] The *k*-space integration was conducted by the tetrahedron method,[35] and the self-consistent charge density was obtained using 468 irreducible *k*-points in the Brillouin zone.

**Table 3.** Selected interatomic distances (Å) for $La_{4.57(1)}Li_{0.43}Ge_{3.80(3)}In_{0.20}$ and $Nd_{4.32(1)}Li_{0.68}Ge_{3.87(3)}In_{0.13}$.

| | Interatomic distance (Å) | |
|---|---|---|
| Atomic pair | $La_{4.57(1)}Li_{0.43}Ge_{3.80(3)}In_{0.20}$ | $Nd_{4.32(1)}Li_{0.68}Ge_{3.87(3)}In_{0.13}$ |
| RE1[a]–RE3[a]/Li (shorter) | 3.6896(11) | 3.5780(19) |
| RE1[a]–RE3[a]/Li (longer) | 3.7541(11) | 3.6395(19) |
| RE2[a]–RE3[a]/Li (shorter) | 3.5888(12) | 3.432(2) |
| RE2[a]–RE3[a]/Li (longer) | 3.6141(12) | 3.492(3) |
| *M*1[b]–*M*1[b] | 2.7131(13) | 2.6863(17) |
| Ge2[b]–*M*3[b] | 2.6365(19) | 2.583(3) |
| *M*1[b]–RE3/Li | 3.3293(10) | 3.2503 (13) |
| Ge2–RE3[a]/Li (shorter) | 3.0294(19) | 2.871(3) |
| Ge2–RE3[a]/Li (longer) | 3.5835(19) | 3.510(3) |
| *M*3[b]–RE3[a]/Li (shorter) | 3.0904(18) | 2.982(3) |
| *M*3[b]–RE3[a]/Li (longer) | 3.1591 (18) | 3.009(3) |

[a] RE = La for $La_{4.57(1)}Li_{0.43}Ge_{3.80(3)}In_{0.20}$; Nd for $Nd_{4.32(1)}Li_{0.68}Ge_{3.87(3)}In_{0.13}$.
[b] *M* = Ge and In mixed-site.

## Results and Discussion

**Crystal Structure Analysis.** Two novel polar intermetallic compounds $La_{4.57(1)}Li_{0.43}Ge_{3.80(3)}In_{0.20}$ and $Nd_{4.32}$

  

$_{(1)}Li_{0.68}Ge_{3.87(3)}In_{0.13}$ were successfully synthesized by the conventional high-temperature synthetic method, and their isotypic crystal structures were characterized by using SXRD analysis. Both title compounds crystallized in the $Gd_5Si_4$-type[24] structure having the orthorhombic space group *Pnma* (Pearson code *oP*16) and six crystallographically independent atomic sites as shown in Tables 1 and 2. Therefore, these two compounds can be considered as quaternary derivatives of $La_5Ge_4$[36] and $Nd_5Ge_4$[37] via the simultaneous Li and In double-doping for rare-earth metals and Ge, respectively.

Since the overall $Gd_5Si_4$-type[24] crystal structure adopted by two title compounds was thoroughly described using two ternary analogues, $La_4LiGe_4$[21] and $Nd_{3.97}Li_{1.03}Ge_4$,[38] in our earlier report, we will be brief for the overall crystal structure using $La_{4.57(1)}Li_{0.43}Ge_{3.80(3)}In_{0.20}$, but rather focus on the "direction selective" structural transformation and the site-preference of In and Ge over three available anionic sites in this article. As illustrated in Figure 1(a), the overall crystal structure of $La_{4.57(1)}Li_{0.43}Ge_{3.8(3)}In_{0.20}$ can be described as the 1:1 assembly of hypothetical 2-dimensioanl (2D) $La_2(La/Li)(Ge/In)_2$ slabs adopting the $Mo_2FeB_2$-type structure and the dumbbell-shaped inter-slabs $(In/Ge)_2$ dimers bridging two such neighboring 2D slabs along the crystallographic *b*-axis direction. In addition, the 2D $La_2(La/Li)(In/Ge)_2$ layer adopting the $Mo_2FeB_2$-type[39] can also be considered as the 1:1 combination of the $La(La_{0.57}Li_{0.43})$ moiety (CsCl-type) and the $La(Ge_{1.95}In_{0.05})$ moiety (AlB2-type). As an alternative view, if we consider the distorted cubic-shaped $La(La_{0.57}Li_{0.43})$ moiety adopting the CsCl-type as a building-block, then the overall crystal structure of $La_{4.57(1)}Li_{0.43}Ge_{3.8(3)}In_{0.20}$ can be illustrated as if the $La(La_{0.57}Li_{0.43})$ units are skewed by the 1D zigzag Ge-La/Li–Ge chains either perpendicular to or along the *ac*-plane directions, respectively, through either the inter-slabs *M*1-*M*1 and the intra-slabs $Ge_2$-$M_3$ dimers as shown in Figure 1(b) and (c). Interestingly, these two types of $M1_2$ or $(Ge_2/M_3)_2$ dimers display two different bond distances: $r(M_1\text{-}M_1)$ = 2.7131 Å and $r(Ge_2\text{-}M_3)$ = 2.6365 Å.

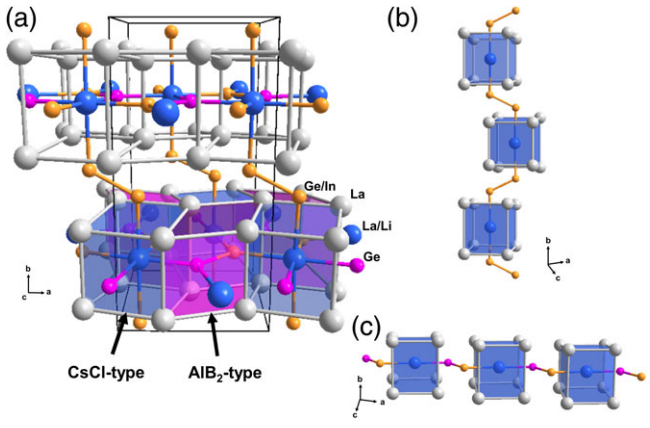


**Figure 1.** Crystal structure of $La_{4.57(1)}Li_{0.43}Ge_{3.80}In_{0.20\ (3)}$ represented by a combination of ball-and-stick and polyhedral representations, viewed from the crystallographic *c*-axis direction. $La(La_{0.57}Li_{0.43})$ (CsCl-type) and $La(Ge_{1.95}In_{0.05})$ ($AlB_2$-type) moieties are highlighted, and a unit cell is outlined. CsCl-type moieties are skewed by the Ge-La/Li–Ge chain either (b) perpendicular to or (c) along the *ac*-plane directions. Color codes: La, gray, La/li mixed-site, blue; Ge/in mixed site, orange; and Ge, magenta.

Some members of the $RE_5M_4$ (RE = rare-earth metals, *M* = triels, tetrels) series adopting the $Gd_5Si_4$-type[24] structure are known to show specific site-preferences of anionic elements, which can be elucidated by the size-factor criterion on the basis of the size match between a central atom and the volume of the given coordinate site. For instance, in the $Gd_5Si_{4-x}Ga_x$ system,[19] the relatively larger-sized Ga prefers to occupy the *M*1 site having the relatively largest-site volume among three anionic sites ($r$(Ga) = 1.26 Å *vs.* $r$(Si) = 1.17 Å).[40] In addition, in the $Gd_5Si_{4-x}M_x$ (*M* = Ge, Sn, and Bi) system,[18,20,41] *M* also tends to occupy the *M*1 site ($r$(Ge) = 1.22 Å, $r$(Sn) = 1.40 Å, and $r$(Bi) = 1.52 Å).[40] There exist some exceptions, which hardly follow this kind of size-factor criterion, such as $Gd_5Si_{4-x}P_x$[42] and $Gd_5Ge_{4-x}P_x$,[43] where the smaller P prefers to occupy the larger *M*1 site ($r$(P) = 1.10 Å).[40] However, these exceptional compounds adopted the $Sm_5Ge_4$-type[23] structure, where the *M*1 atoms were considered as terminal atoms. Therefore, the electronic-factor criterion based on the QVALs and the electronegativities of elements should be applied to understand the given site preference. In general, the QVAL of each site is evaluated by the summation of integrated electron densities inside each corresponding WS sphere. Thus, we should expect an element having the higher electronegativity to occupy an atomic site with the larger QVAL. The two title compounds in this article also follow the electronic-factor criterion based on these QVALs and electronegativities of elements occupying the site rather than the size-factor criterion (Figure S2). For instance, in $La_{4.57(1)}Li_{0.43}Ge_{3.80(3)}In_{0.20}$, 8% and 5% of In substitutions are observed at the *M*1 and *M*3 sites, respectively. Moreover, in $Nd_{4.32(1)}Li_{0.68}Ge_{3.87(3)}In_{0.13}$, these two anionic sites *M*1 and *M*3 are still preferred by In as shown in Table 2 (4% *vs.* 6%). Since the overall amounts of substituting In in two title compounds are rather small, it would be hard to concretely choose the most preferred site by In among three available anionic sites. However, it is very clear that the *M*2 site includes no In substitution at all. This type of site-preference of the anionic In atom will be further discussed in Electronic Structure section using results of theoretical investigations.

Interestingly, these two quaternary compounds can be considered as products of structural transformation from the $Sm_5Ge_4$-type[23] to the $Gd_5Si_4$-type[24] structure via the simultaneous In and Li double-doping. The changes of interatomic distances among $La_5Ge_4$, $La_4LiGe_4$, and $La_{4.57(1)}Li_{0.43}Ge_{3.80(3)}In_{0.20}$ are nicely compared in Figure 2. In our earlier report for the $RE_4LiGe_4$ (RE = La, Ce, Pr, Sm) system,[21] as the substituting Li replaced RE at the RE3 site in the parental $RE_5Ge_4$, the lattice parameter *a* decreased

  

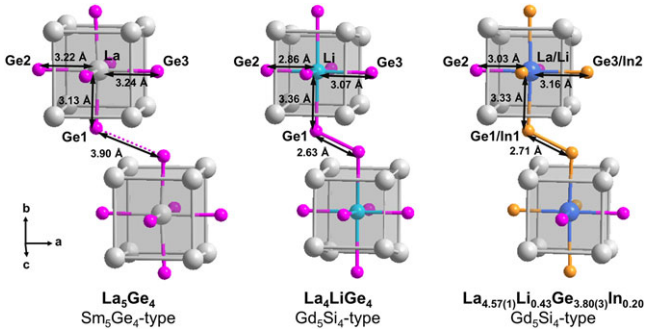


**Figure 2.** A schematic illustration of comparing the local coordinate geometries among $La_5Ge_4$ ($Sm_5Ge_4$-type), $La_4LiGe_4$ ($Gd_5Si_4$-type) and $La_{4.57(1)}Li_{0.43}Ge_{3.80(3)}In_{0.20}$ ($Gd_5Si_4$-type). Selected interatomic distances are also provided. More detailed description can be found in the text.

significantly, whereas lattice parameter *b* and *c* were nearly intact. This type of "direction selective" structural transformation was caused by the chemical pressure applied only along the *a*-axis direction, which was originally triggered by the Li substitution for RE at the RE3 site and the resultant formation of inter-slabs $Ge_2$ dimers. In the current quaternary La compound, $La_{4.57(1)}Li_{0.43}Ge_{3.80(3)}In_{0.20}$, the two lattice parameters *b* and *c* are noticeably longer than those of $La_5Ge_4$[36] as well as $La_4LiGe_4$,[21] but the lattice parameter *a* is shorter than that of $La_5Ge_4$: 8.076 Å ($La_5Ge_4$) > 7.828 Å ($La_{4.57(1)}Li_{0.43}Ge_{3.80(3)}In_{0.20}$) > 7.596 Å ($La_4LiGe_4$). Firstly, this kind of direction selective structural transformation can be understood by the relatively smaller amount of Li substitution for La at the RE3 site in $La_{4.57(1)}Li_{0.43}Ge_{3.80(3)}In_{0.20}$ compared to that in the $La_4LiGe_4$.[21] In other words, the amount of Li in $La_{4.57(1)}Li_{0.43}Ge_{3.80(3)}In_{0.20}$ is sufficient to transform the structural type from the $Sm_5Ge_4$-type[23] to the $Gd_5Si_4$-type,[24] but not enough to make the lattice parameter *a* as short as that in $La_4LiGe_4$.[21] Secondly, the elongated lattice parameters *b* and *c* can be attributed to the relatively larger-sized In substitution for Ge ($r$(In) = 1.50 Å, $r$(Ge) = 1.22 Å)[40] at both of the *M*1 and *M*3 sites. As a result, the inter-slabs *M*1-*M*1 dimer is formed due to the successful Li substitution at the RE3 site in the La-containing title compound, but the actual *M*1-*M*1 distance is longer than that of Ge1-Ge1 in $La_4LiGe_4$[21] due to the partial In substitution at the *M*1 site. In addition, we can conclude that the In substitution at the *M*3 site also causes a certain degree of volume expansion of the 2D $La_2(La/Li)(Ge/In)_2$ slab, which eventually results in lengthening of the lattice parameter *b* and *c* of a unit cell.

**Electronic Structure and Chemical Bonding.** To understand the site-preference of In among three available anionic sites and the overall electronic structure including chemical bonding of two title compounds, we conducted a series of theoretical calculations using four hypothetical structural models by the TB-LMTO-ASA method.[29–33] According to our SXRD refinements for two title compounds, the substituting In was found at both of the *M*1 and *M*3 sites with slightly different mixed-occupational ratios to Ge, but no In was detected at the *M*2 site as provided in Table 2.

Therefore, we designed four distinctive structural models containing In at the four different sites in each unit cell (see Figure 3). Since the crystal structures of two title compounds are isotypic, we decided to use the La compound as a representative for the following theoretical calculations. For practical reasons, an idealized composition of $La_4LiGe_3In$ was applied for these models, and lattice parameters and atomic coordinates were extracted from the SXRD data of $La_{4.57(1)}Li_{0.43}Ge_{3.80(3)}In_{0.20}$. In particular for Models 1 and 2, two different atomic arrangements between In and Ge along the *b*-axis direction are applied as In is introduced to the *M*1 site. Therefore, two subgroups $P2_12_12_1$ (No. 19) and $P2_1/m$ (No. 11) of the refined space group *Pnma* were adopted to apply alternating arrangements of either In and Ge or $In_2$ and $Ge_2$ along the *b*-axis direction in Model 1 and Model 2, respectively. For Models 3 and 4, the experimentally determined space group *Pnma* (No. 62) was just exploited, and the substituting In was located at the *M*2 and *M*3 site, respectively. Further details about structural information of these models are provided in Table S1.

The results of a series of theoretical calculations proved that Model 4 having In at the *M*3 site is energetically the most favorable structure among four models. Model 1 containing In at the *M*1 site with an alternating atomic arrangement with Ge is the next favorable structure, and it shows

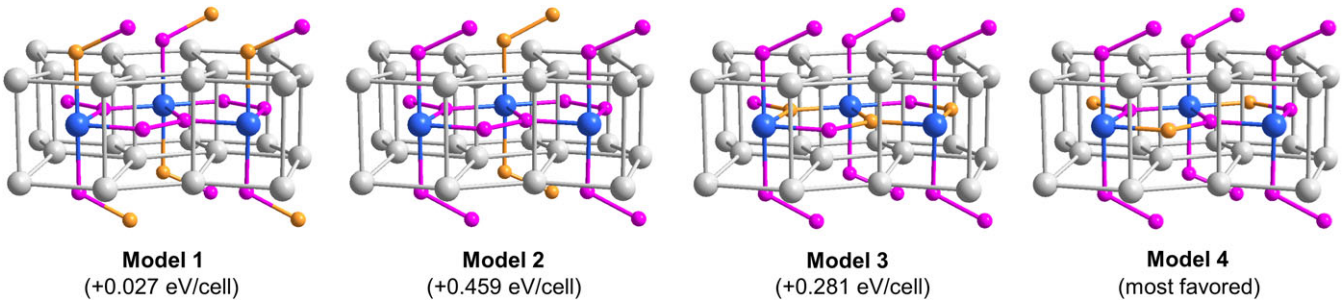


**Figure 3.** Four hypothetical structural modes of $La_4LiGe_3In$ having different in sites. The relative total electronic energy differences are also provided. More detailed description about each model can be found in the text. Color codes: La, gray, La/li mixed-site, blue; Ge, magenta; and in, orange.

  

the slightly higher total electronic energy (+ 0.027 eV/cell) than Model 4. However, as we mentioned in *Crystal Structure Analysis*, due to the rather slight difference of the mixed occupation of In at the *M*1 and the *M*3 sites, the in site preference between these two anionic sites is hardly distinguishable. Interestingly, Model 2 also containing In at the *M*1 site as a form of $In_2$ dimer shows the significantly higher total electronic energy than Model 1 (+ 0.459 eV/cell) as well as two other models. This proves that the inter-slabs $In_2$ dimers connecting two neighboring 2D $La_2(La/Li)(Ge/In)_2$ slabs used in Model 2 seem to be least plausible. In addition, Model 3 containing In at the *M*2 site also shows the rather larger electronic energy than Model 1 (+ 0.281 eV/cell) and Model 4. Therefore, we can see that these results of theoretical investigations are in good agreements with the SXRD results, where no In is refined at the *M*2 site in the title compounds.

To understand an overall electronic structure and chemical bonding between anionic elements of $La_{4.57(1)}Li_{0.43}Ge_{3.80(3)}In_{0.20}$, the DOS and COHP curves calculated using Model 4 analyses were thoroughly interrogated. The overall DOS curve displayed in Figure 4(a) can be divided into four sections: (1) the region between ca. -9.2 and − 7.8 eV shows two sharp peaks mostly contributed by 4s and 5s orbitals of Ge and In forming $\sigma$ bonding interactions in two different type of $(Ge/In)_2$ dimers, *e.g.,* either inter-slabs or intra-slabs; (2) the region between ca. -7 and −5 eV also shows two peaks contributed mostly by 4s and 5s orbitals of Ge and In as well, but forming $\sigma^*$ antibonding interactions; (3) the region between ca. -3.5 and 0 eV displays complex orbital mixing of La 6s and 5d, Li 2s, Ge 4p, and In 5p states; and (4) the region beyond $E_F$ contains major contributions from La 6s and 5d states. Interestingly, the low-end peak observed at ca. -9 eV presents the major contribution from the intra-slabs $(Ge/In)_2$ dimers having a bond distance of 2.637 Å, whereas the peak at ca. -8 eV contains the largest contribution from the inter-slabs $(Ge/In)_2$ dimers with a distance of 2.713 Å. Figure 4 (b) shows two COHP curves representing interatomic interactions of the intra-slabs as well as inter-slabs $(Ge/In)_2$ dimers. Interestingly, the Ge1-In1 COHP curve indicating the inter-slabs interactions shows a significantly decreased antibonding character around $E_F$ comparing to that of the Ge1-Ge1 COHP curve in $La_4LiGe_4$[21] provided in Figure S3. This type of reduced antibonding character of a particular chemical bonding makes the overall crystal structure energetically more favorable. In addition, we also provided another $E_F$ at ca. + 0.5 eV corresponding to the experimentally refined chemical composition with 29.94 $ve^-$. It proves that these two particular interatomic interactions of intra-slab dimers maintain nearly non-bonding interactions up to the new $E_F$. Therefore, the electronic structure analysis also indicates that the refined chemical composition $La_{4.57(1)}Li_{0.43}Ge_{3.80(3)}In_{0.20}$ contains no additional unfavorable antibonding interactions.

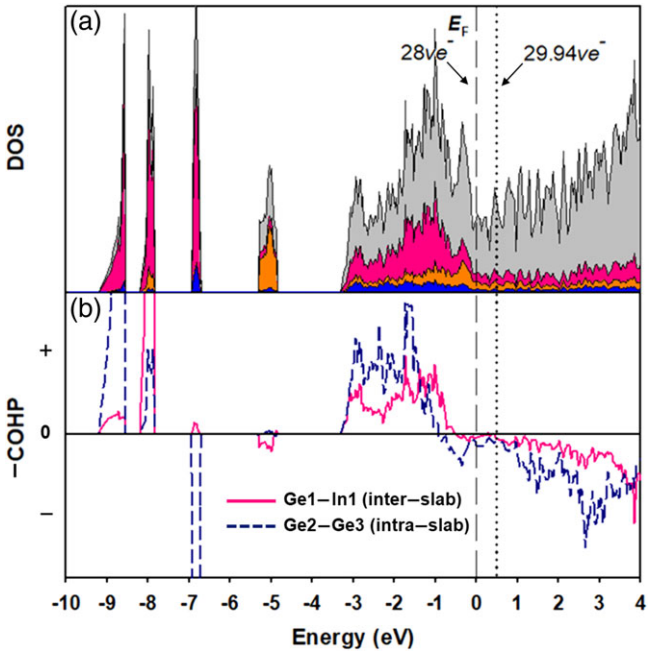


**Figure 4.** DOS and COHP curves of $La_4LiGe_3In$ based on the model 4. (a) Total DOS (black outline), La PDOS (gray region), li PDOS (blue region), Ge PDOS (magenta region), and in PDOS (orange region). Two COHP curves represent interatomic interactions for (b) the inter-slab (Ge1-In1) dimers and the intra-slab (Ge2-Ge3) dimers. $E_F$ (vertical dashed-line) is the energy reference (0 eV). The number of valence electron concentrations for two Fermi levels corresponding to the experimentally refined (29.94 $ve^-$) and the idealized compositions (28 $ve^-$) are also provided. The region with the "+" sign represent bonding interactions, whereas the region with "–" sign represents antibonding interactions.

## Conclusion

Two novel quaternary polar intermetallic compounds, $La_{4.57(1)}Li_{0.43}Ge_{3.80(3)}In_{0.20}$ and $Nd_{4.32(1)}Li_{0.68}Ge_{3.87(3)}In_{0.13}$, which can be considered as quaternary derivatives of two binary parent compounds $La_5Ge_4$ and $Nd_5Ge_4$ via the Li and In double-doping, were successfully synthesized by high-temperature reaction method. The isotypic $Gd_5Si_4$-type crystal structure of the two title compounds can be described as the 1:1 assembly of the $Mo_2FeB_2$-type 2D $La_2(La/Li)(Ge/In)_2$ slabs and the bridging inter-slabs $(Ge/In)_2$ dimers. The "direction selective" structural transformation from the $Sm_5Ge_4$-type to the $Gd_5Si_4$-type in our title compounds was triggered by the simultaneous double-doping of Li and In for the *RE*3 site and Ge, respectively. In particular, the substituting In specifically occupied the *M*1 and *M*3 sites, and this kind of particular site-preference of In can be explained by electronic-factor criterion on the basis of QVAL of each site. A series of theoretical calculations using four different hypothetical $La_3LiGe_3In$ models proves that the models having In at the *M*3 and *M*1 sites are energetically more favorable than the models having In at the *M*2 site and the *M*1 site in the form of inter-slabs $In_2$

  

dimers, which are in good agreements with experimental results. The Ge1-In1 COHP curve of a representative $La_4LiGe_3In$ model, which presents the inter-slab interaction, indicates a significantly decreased antibonding character around $E_F$ comparing to that of the Ge1-Ge1 COHP curve in $La_4LiGe_4$, and this type of reduced antibonding character indicates energetically the more stabilized overall crystal structure.

**Acknowledgments.** This research is supported by Basic Science Research Program through NRF funded by the Ministry of Science, ICT and Future Planning (NRF-2015R1A1A1A05027845).

**Supporting Information.** Additional supporting information may be found online in the Supporting Information section at the end of the article.

## References

1. V. K. Percharsky, K. A. Gschneidner Jr. , *Phys. Rev. Lett.* **1997**, *78*, 4494.
2. Y. Mozharivskyj, A. O. Pecharsky, V. K. Pecharsky, G. J. Miller, *J. Am. Chem. Soc.* **2005**, *127*, 317.
3. H. Wang, F. Wang, K. Jones, G. J. Miller, *Inorg. Chem.* **2011**, *50*, 12714.
4. L.-M. Wu, S.-H. Kim, D.-K. Seo, *J. Am. Chem. Soc.* **2005**, *127*, 15682.
5. H. Wang, S. Misra, F. Wang, G. J. Miller, *Inorg. Chem.* **2010**, *49*, 4586.
6. V. K. Pecharsky, K. A. Gschneidner Jr. , *Appl. Phys. Lett.* **1997**, *70*, 3299.
7. J. Yao, P. Wang, Y. Mozharivskyj, *Chem. Mater.* **2012**, *24*, 552.
8. J. Yao, P. Lyutyy, Y. Mozharivskyj, *Dalton Trans.* **2011**, *40*, 4275.
9. S. Misra, E. T. Poweleit, G. J. Miller, *Z. Anorg. Allg. Chem.* **2009**, *635*, 889.
10. S. Misra, G. J. Miller, *J. Am. Chem. Soc.* **2008**, *130*, 13900.
11. J. M. Elbicki, L. Y. Zhang, R. T. Obermyer, W. E. Wallace, S. G. Sankar, *J. Appl. Phys.* **1991**, *69*, 5571.
12. Y. Mudryk, D. Paudyal, V. K. Pecharsky, K. A. Gschneidner Jr. , S. Misra, G. J. Miller, *Phys. Rev. Lett.* **2010**, *105*, 066401.
13. J. Yao, P. L. Wang, Y. J. Mozharivskyj, *Alloys Compd.* **2012**, *534*, 74.
14. J. Yao, Y. Z. Mozharivskyj, *Z. Anorg. Allg. Chem.* **2011**, *637*, 2039.
15. P. H. Tobash, S. Bobev, J. D. Thompson, J. L. Sarrao, *Inorg. Chem.* **2009**, *48*, 6641.
16. W. Choe, G. J. Miller, J. Meyers, S. Chumbley, A. O. Pecharsky, *Chem. Mater.* **2003**, *15*, 1413.
17. A. O. Pecharsky, K. A. Gschneidner, V. K. Pecharsky, C. E. Schindler, *J. Alloys Compd.* **2002**, *338*, 126.
18. W. Choe, A. O. Pecharsky, M. Wörle, G. J. Miller, *Inorg. Chem.* **2003**, *42*, 8223.
19. Y. Mozharivskyj, W. Choe, A. O. Pecharsky, G. J. Miller, *J. Am. Chem.* **2003**, *125*, 15183.
20. Y. Mozharivskyj, A. O. Tsokol, G. J. Miller, *Z. Kristallogr.* **2006**, *221*, 493.
21. G. Nam, J. Jeon, Y. Kim, S. Kang, K. Ahn, T.-S. You, *J. Solid State Chem.* **2013**, *205*, 10.
22. G. J. Miller, *J. Eur. Inorg. Chem.* **1998**, *1998*, 523.
23. G. S. Smith, Q. Johnson, A. G. Tharp, *Acta Crystallogr.* **1967**, *22*, 269.
24. J. E. Iglesias, H. J. Steinfink, *Less-Common Met* **1972**, *26*, 45.
25. Bruker, *APEX2*, Bruker AXS Inc, Madison, WI, **2007**.
26. Bruker, *SAINT*, Bruker AXS Inc, Madison, WI, **2002**.
27. G. M. Sheldrick, *SADABS*, University of Göttingen, Göttingen, **2003**.
28. L. M. Gelato, E. Parthé, *J. Appl. Crystallogr.* **1987**, *20*, 139.
29. O. K. Andersen, *Phys. Rev. B* **1975**, *12*, 3060.
30. O. K. Andersen, O. Jepsen, *Phys. Rev. Lett.* **1984**, *53*, 2571.
31. O. K. Andersen, *Phys. Rev. B* **1986**, *34*, 2439.
32. O. Jepsen, A. Burkhardt, O. K. Andersen, *The TB-LMTO-ASA Program, Version 4.7*, Max-Plank-Institut fur Festkorperforschung, Shuttgart, **1999**.
33. O. K. Andersen, O. Jepsen, D. Glötzel, In *Highlights of Condensed Matter Theory*, F. Bassani, F. Fumi, M. Tosi Eds., North Holland, New York, NY, **1985**.
34. O. Jepsen, O. K. Andersen, *Z. Phys. B Condens. Matter* **1995**, *97*, 35.
35. P. E. Blöchl, O. Jepsen, O. K. Andersen, *Phys. Rev. B* **1994**, *49*, 16223.
36. H. F. Yang, G. H. Rao, G. Y. Liua, Z. W. Ouyang, W. F. Liu, X. M. Feng, W. G. Chu, J. K. Liang, *J. Alloys Compd.* **2003**, *361*, 113.
37. H. F. Yang, G. H. Rao, G. Y. Liua, Z. W. Ouyang, W. F. Liu, X. M. Feng, W. G. Chu, J. K. Liang, *J. Alloys Compd.* **2002**, *346*, 190.
38. N. T. Suen, T.-S. You, S. Bobev, *Acta Crystallogr. Sect. C: Cryst. Struct. Commun.* **2013**, *69*, 1.
39. W. Choe, G. J. Miller, E. M. Levin, *J. Alloys Compd.* **2001**, *329*, 121.
40. J. Emsley, *The Elements*, Oxford University Press, New York, NY, **1989**.
41. V. Svitlyk, B. J. Campbell, Y. Mozharivskyj, *Inorg. Chem.* **2009**, *48*, 10364.
42. V. Svitlyk, Y. Mozharivskyj, *Solid State Sci.* **2009**, *11*, 1941.
43. Y. Y. J. Cheung, V. Svitlyk, Y. Mozharivskyj, *J. Magn. Magn. Mater.* **2013**, *331*, 237.

  